

RI 7854

Bureau of Mines Report of Investigations/1974

**Dispersion of Dust in a Channel
by a Turbulent Gas Stream**



UNITED STATES DEPARTMENT OF THE INTERIOR

Report of Investigations 7854

Dispersion of Dust in a Channel by a Turbulent Gas Stream

**By C. C. Hwang, J. M. Singer, and T. N. Hartz
Pittsburgh Mining and Safety Research Center, Pittsburgh, Pa.**



**UNITED STATES DEPARTMENT OF THE INTERIOR
Rogers C. B. Morton, Secretary**

**BUREAU OF MINES
Thomas V. Falkie, Director**

This publication has been cataloged as follows:

Hwang, C C

Dispersion of dust in a channel by a turbulent gas stream,
by C. C. Hwang, J. M. Singer, and T. N. Hartz. [Washing-
ton] U.S. Bureau of Mines [1974]

29 p. illus., tables. (U.S. Bureau of Mines. Report of investi-
gations 7854)

1. Mine dusts. 2. Mine explosions. I. U.S. Bureau of Mines.
II. Singer, Joseph Marcus, 1918- , jt. auth. III. Hartz, T. N.,
jt. auth. IV. Title. (Series)

TN23.U7 no. 7854 622.06173

U.S. Dept. of the Int. Library

CONTENTS

	<u>Page</u>
Abstract.....	1
Introduction.....	1
Acknowledgments.....	2
General formulation.....	2
Analysis.....	5
The case of a circular cross section.....	5
The case of rectangular cross sections.....	8
Results.....	11
Experimental data used in computations.....	11
Results of computations and discussion.....	14
Summary.....	27
Appendix.--List of symbols.....	28

ILLUSTRATIONS

1. Coordinate system for the case of a circular cross section.....	3
2. Coordinate system for the case of rectangular cross sections.....	4
3. Cylindrical dust bed configuration.....	4
4. Rectangular dust bed configuration.....	4
5. Regression of leading edge of rock dust bed.....	6
6. Dust concentration as a function of distance from wall in a square channel at $t = 0.1$ sec.....	14
7. Dust concentration in a square channel at $t = 0.2$ sec.....	15
8. Dust concentration in a square channel at $t = 0.3$ sec.....	16
9. Dust concentration in a square channel at $t = 1.0$ sec.....	17
10. Dust concentration in a square and a circular channel as a function of distance from wall at $t = 0.1$ sec.....	18
11. Dust concentration in a square and a circular channel as a function of distance from wall at $t = 0.3$ sec.....	18

TABLES

1. The effect of the diffusion coefficient, k , on rock dust concentration.....	20
2. The effect of velocity on rock dust concentration.....	21
3. Surface lifting versus line source lifting of rock dust.....	22
4. Surface lifting of 0.32-cm beds from side and roof, and line source lifting of 1.25-cm rock dust beds from floor.....	23
5. Surface lifting of top 0.32 cm of coal layer and line source lifting of underlying 1.25 cm of rock dust layer.....	25
6. Surface dispersal of mixture of 65 percent rock dust and 35 percent coal dust.....	26

DISPERSION OF DUST IN A CHANNEL BY A TURBULENT GAS STREAM

by

C. C. Hwang,¹ J. M. Singer,² and T. N. Hartz³

ABSTRACT

The Bureau of Mines formulated a method for calculating the concentration of entrained dust from a dust deposit by a turbulent gas stream. In particular, a diffusion equation is used to calculate dust concentrations in a channel following an explosion.

Dust leaving the channel walls was treated as originating from stationary or moving, and single or multiple material sources. Formulas and sample computations for various types of dust sources in circular and rectangular channels are given, based on experimental entrainment rates.

The analysis predicts the dust concentration as a function of time and channel space. The results appear to agree with the physical characteristics of explosion-driven dust dispersion in a 0.6-m-diameter, 50-m-long explosion tunnel. The analysis is also applied to simultaneous and consecutive dispersion of coal and rock dust from simulated coal mine surfaces (walls, floor, roof, and ribs).

INTRODUCTION

In explosions of coal mine dust and gas, the turbulent gas stream induced by the explosion disperses dust from the mine entry walls into the stream, allowing the explosion to sustain itself and propagate through the entry. The concentration of dust in the gas stream ahead of the explosion is one of the parameters which determines subsequent explosion and flame-propagation characteristics. The objective of this Bureau of Mines study was to predict dust concentrations in the flowing airstream induced by the initial explosion as a function of time and space.

The formation of the float-coal-dust cloud in an explosion may be divided into the two following steps: (1) Dust is lifted from the entry walls by the gas stream; and (2) the dust is dispersed by turbulent transport processes.

¹Mechanical engineer (Faculty Member at University of Pittsburgh).

²Research chemist.

³Mathematician.

At present there is no general experimental correlation, or theory, that predicts the amount of dust removed under given flow and dust bed conditions, although some experimental effort has been made in this direction.⁴ However, it is with the second step that the present paper is concerned. The process of turbulent mixing has been treated as a diffusion process, using diffusion-type equations that have been successfully applied to the dispersion of matter in pipes (solute, particles), open channels (sediment), and semi-infinite domains (air pollutants). In the analysis which follows, the diffusion equation contains arbitrary but typical turbulent diffusion coefficients; and the dust leaving the walls is treated as originating from stationary or moving sources. The entrainment rates of dust leaving the walls are assumed to be known from experiments. Both circular and rectangular channel cross sections are considered. Several sequential and simultaneous modes of entrainment typical of dust dispersion in coal mine explosions are examined, with coal and rock dust beds as the material sources that are dispersed into the turbulent gas stream. It is emphasized here that the method presented in this report is a first step toward solving more complex problems.

Specifically, the present method is limited to the case of (1) constant, one-dimensional convective velocity, (2) negligible gravity, and (3) constant diffusion coefficient.

ACKNOWLEDGMENTS

The authors are grateful to Dr. Donald Chi, research physicist, for his assistance in computer programming, and to Joseph Grumer, supervisory research chemist, for his helpful discussion during the course of this work.

GENERAL FORMULATION

Consider a channel of circular or rectangular cross section, for which the coordinate systems are shown, respectively, in figures 1 and 2. The shapes of the corresponding dust beds are in figures 3 and 4. The gas flows in the positive z direction. If c is the dust concentration, the diffusion equation can be written as⁵

$$\frac{\partial c}{\partial t} + \bar{U} \cdot \text{grad } c = \text{div } (k \text{ grad } c), \quad (1)$$

⁴Dawes, J. G. Dispersion of Dust Deposits by Blasts of Air. Part 1, Safety in Mines Res. Establishment Res. Rept. 36, 1952, 69 pp.

Dawes, J. G. Dispersion of Dust Deposits by Blasts of Air. Part 2, Safety in Mines Res. Establishment Res. Rept. 49, 1952, 44 pp.

Singer, J. M., N. B. Greninger, and J. Grumer. Some Aspects of the Aerodynamics of Formation of Float Coal Dust Clouds. BuMines RI 7252, 1969, 26 pp.

Singer, J. M., E. Cook, and J. Grumer. Dispersal of Coal- and Rock-Dust Deposits. BuMines RI 7642, 1972, 32 pp.

⁵Rohsenow, W. M., and H. Choi. Ch. in Heat, Mass, and Momentum Transfer, Prentice-Hall, Inc., Englewood Cliffs, N.J., 1963, pp. 387-409.

$\hat{r}, \hat{\theta}, \hat{z}$ are unit vectors in r, θ, z directions respectively

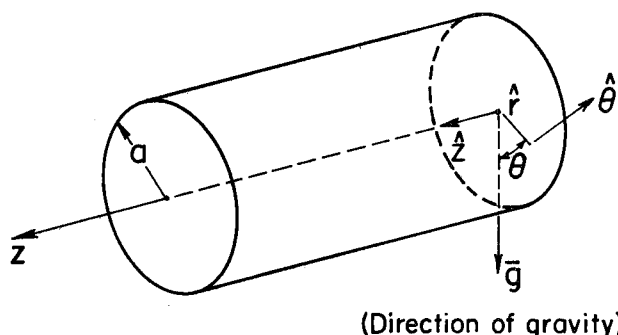


FIGURE 1. - Coordinate system for the case of a circular cross section.

neglected in the initial period of the dispersion process and that the gross behavior of the dust cloud is dictated by diffusion equation 1 with appropriate values of k . In an actual explosion, the gas velocity may reverse its direction because of pressure wave interactions; the present analysis will be limited to the initial period of the process when \bar{U} is in the positive z direction. To express the condition of no loss through the channel walls, the boundary condition must satisfy the equation

$$k \left. \frac{\partial c}{\partial n} \right|_{\text{wall}} = 0, \quad (2)$$

where n signifies the direction normal to the wall. The initial dust concentration in the gas is assumed to be zero.

Experimental observations show that dust is dispersed into the gas stream from the channel walls by erosion and denudation.⁶ To model these processes, equation 1 will be solved for the following cases:

- a. A stationary point source on the channel wall;
- b. a stationary line source on the channel wall and on the plane perpendicular to the gas stream;
- c. the line source in b moving with a prescribed velocity in the direction of the gas stream, and
- d. a stationary surface source covering the area of the dust bed (figs. 3-4).

⁶Footnote 4 parts 2 and 3 show that the major entrainment mode of cohesive rock and coal dust deposits is denudation in which aggregates and clumps are fragmented from the leading edge and finally dispersed in midstream.

where k is the diffusion coefficient, and $\bar{U} = \bar{U}(\bar{x}, t)$ is the convection velocity with which the dust is convected in addition to being diffused. In general, \bar{U} is different from the gas velocity because of the inertia of the dust particles in the flow. In the present analysis \bar{U} is taken in the axial direction and is constant in magnitude. This condition does not allow for effect of gravity which causes dust particles to precipitate. It is assumed that the effect of gravity may be

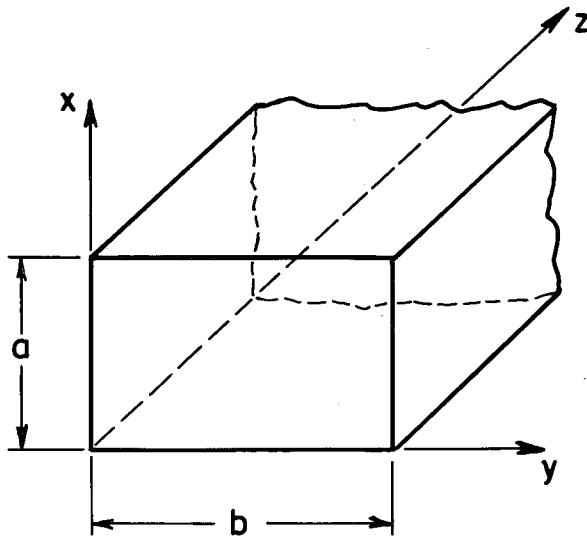


FIGURE 2. - Coordinate system for the case of rectangular cross sections.

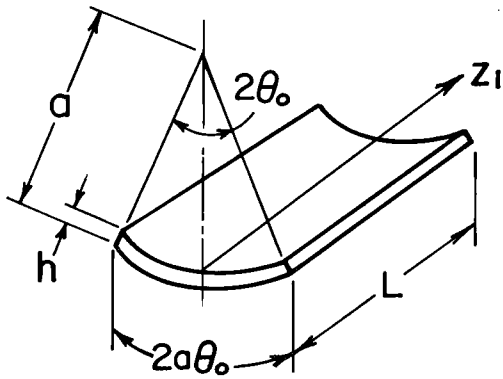


FIGURE 3. - Cylindrical dust bed configuration.

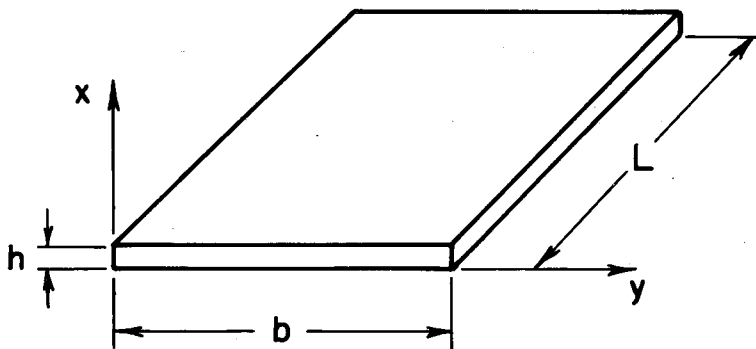


FIGURE 4. - Rectangular dust bed configuration.

Because the governing equation 1 is linear, the solutions of a through d can be superimposed to give an appropriate distribution as observed in experiments.

ANALYSIS

The Case of a Circular Cross Section

Using the cylindrical coordinate system as shown in figure 1, equation 1 can be written,

$$\frac{\partial c}{\partial t} + U \frac{\partial c}{\partial z} = k \left[\frac{1}{r} \frac{\partial}{\partial r} \left(r \frac{\partial c}{\partial r} \right) + \frac{1}{r^2} \frac{\partial^2 c}{\partial \theta^2} + \frac{\partial^2 c}{\partial z^2} \right]. \quad (3)$$

The convection term in the above equation can be eliminated through a coordinate transformation

$$Z = z - Ut, \quad (4)$$

and equation 3 becomes

$$\frac{1}{r} \frac{\partial}{\partial r} \left(r \frac{\partial c}{\partial r} \right) + \frac{1}{r^2} \frac{\partial^2 c}{\partial \theta^2} + \frac{\partial^2 c}{\partial Z^2} = \frac{1}{k} \frac{\partial c}{\partial t}. \quad (5)$$

For the case of an instantaneous point source Q (mass of dust production) at $t = 0$ at the point $(r_1, \theta_1, 0)$, and no loss of mass at the boundary, that is,

$$k \frac{\partial c}{\partial r} \Big|_{r=a} = 0, \quad (6)$$

the solution is found to be⁷

$$c = \frac{Q e^{-z/4kt}}{2\pi a^2 \sqrt{\pi kt}} \left[1 + \sum_{n=-\infty}^{\infty} \cos n(\theta - \theta_1) \cdot \sum_{\alpha} e^{-k\alpha^2 t} \frac{\alpha^2 J_n(\alpha r) J_n(\alpha r_1)}{[\alpha^2 - (n^2/a^2)] J_n^2(a\alpha)} \right], \quad (7)$$

where the summation in α is over the positive roots of

$$\frac{d}{dr} J_n(\alpha r) \Big|_{r=a} = 0. \quad (8)$$

Jordan⁸ has treated the case for which the diffusion coefficient in the radial direction is different from that in the axial direction. The analysis is very similar to the one just described.

The next step is to find an expression for $c(r, \theta, z, t)$ with an instantaneous point source at $t = t_1$ at the point (a, θ_1, z_1) . This is done by

⁷Carslaw, H. S., and J. C. Jaeger. Conduction of Heat in Solids. Oxford University Press (London), 2d ed., 1960, p. 378.

⁸Jordan, D. W. A Theoretical Study of the Turbulent Diffusion of Tracer Gas in Airways. Quart. J. Mech. Appl. Math., v. 14, pt. 2, 1961, pp. 203-222.

replacing r_1 , Z , and t in equation 7 by a , $(z-z_1)-U(t-t_1)$, and $(t-t_1)$, respectively:

$$c = \frac{Qe^{-[(z-z_1)-U(t-t_1)]^2/4k(t-t_1)}}{2\pi a^2 \sqrt{\pi k(t-t_1)}} \cdot \left[1 + \sum_{n=-\infty}^{\infty} \cos n(\theta-\theta_1) \sum_{\alpha} e^{-k\alpha^2(t-t_1)} \frac{\alpha^2 J_n(\alpha r)}{[\alpha^2 - (n^2/a^2)] J_n(\alpha a)} \right]. \quad (9)$$

The width of the dust pile is assumed to extend from $\theta = -\theta_0$ to $+\theta_0$ at $r = a$ (fig. 2). A continuous distribution of instantaneous point sources along $r = a$, $-\theta_0 \leq \theta \leq \theta_0$ is equivalent to an instantaneous circular-arc source, and the expression can be obtained by integrating equation 9 with respect to θ_1 from $-\theta_0$ to θ_0 :

$$c = \frac{2\theta_0 Q e^{-[(z-z_1)-U(t-t_1)]^2/4k(t-t_1)}}{2\pi^{3/2} a^2 \sqrt{k(t-t_1)}} \left[1 + \sum_{n=-\infty}^{\infty} \frac{1}{n\theta_0} \sin(n\theta_0) \cos(n\theta) \cdot \sum_{\alpha} e^{-k\alpha^2(t-t_1)} \frac{\alpha^2 J_n(\alpha r)}{(\alpha^2 - n^2/a^2) J_n(\alpha a)} \right]. \quad (10)$$

Now consider a dust bed of length L and width (arc length) $2a\theta_0$ on the wall of the channel (fig. 3). When the bed is denuded by the forces exerted by a gas stream, the process is observed to start at the leading edge of the bed and proceed downstream. It is proposed to replace this regressing leading edge by a moving source, $Q_1(t_1)dt_1$ (a line source of circular arc shape),

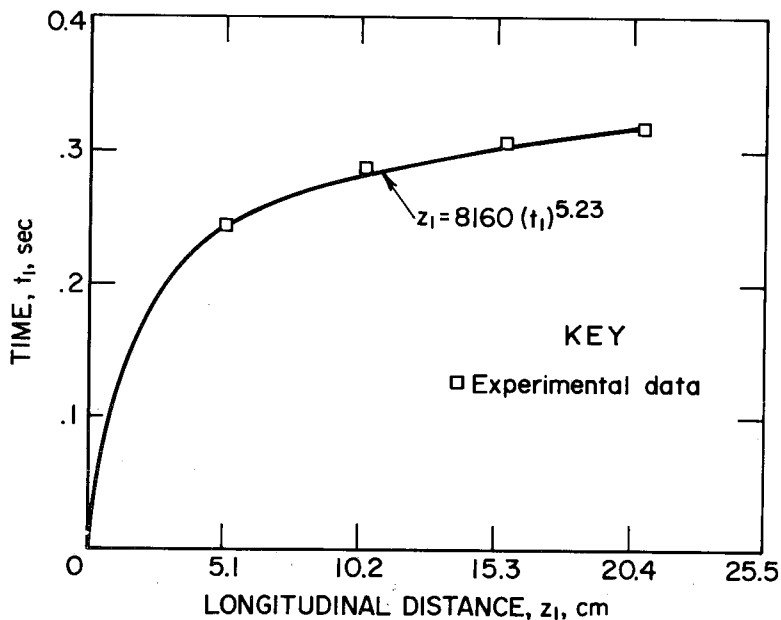


FIGURE 5. - Regression of leading edge of rock dust bed (typical example).

$Q_1(t_1)$ being the mass rate of production of the line source. It is observed experimentally that the regression speed of a dust bed increases with time under explosion-source conditions. A typical curve relating the leading edge of a regressed dust bed z_1 , and the elapsed time t_1 is shown in figure 5.⁹ The

⁹Derived from data being developed on explosion driven dust dispersion in a 0.6-m-diameter, 50-m-long explosion tunnel, by J. M. Singer, M. G. Harris, and J. Grumer at the Pittsburgh Mining and Safety Research Center.

$z_1 - t_1$ relation is approximated by the relation

$$z_1 = Mt_1^N. \quad (11)$$

The regression speed is obtained by differentiating z_1 with respect to t_1 ,

$$\frac{dz_1}{dt_1} = MNt_1^{N-1}, \quad (12)$$

$Q_1(t_1)dt_1$ can be expressed by

$$\begin{aligned} Q_1(t_1)dt_1 &= \rho \cdot 2a\theta_0 \cdot h \cdot \frac{dz_1}{dt_1} dt_1 \\ &= \rho \cdot 2a\theta_0 \cdot h \cdot MNt_1^{N-1} dt_1, \end{aligned} \quad (13)$$

where ρ is the bulk density of the bed. The dust concentration $c(r, \theta, z, t)$ resulting from this moving line source can be obtained by replacing $2\theta_0 Q$ in equation 10 by equation 13 and integrating the resulting expression with respect to t_1 .

For the case $t < \tau$,

$$\begin{aligned} c &= \frac{2\rho a\theta_0 hMN}{2\pi^{3/2} a^2 \sqrt{k}} \int_0^t \frac{t_1^{N-1} e^{-[(z-z_1)-U(t-t_1)]^2/4k(t-t_1)}}{\sqrt{t-t_1}} \cdot \left[1 \right. \\ &\quad \left. + \sum_{n=-\infty}^{\infty} \frac{1}{n\theta_0} \sin(n\theta_0) \cos(n\theta) \sum_{\alpha} e^{-k\alpha^2(t-t_1)} \frac{\alpha^2 J_n(\alpha r)}{(\alpha^2 - n^2/a^2) J_n(\alpha a)} \right] dt_1, \end{aligned} \quad (14)$$

for the case $t \geq \tau$,

$$\begin{aligned} c &= \frac{2\rho a\theta_0 hMN}{2\pi^{3/2} a^2 \sqrt{k}} \int_0^{\tau} \frac{t_1^{N-1} e^{-[(z-z_1)-U(t-t_1)]^2/4k(t-t_1)}}{\sqrt{t-t_1}} \cdot \left[1 \right. \\ &\quad \left. + \sum_{n=-\infty}^{\infty} \frac{1}{n\theta_0} \sin(n\theta_0) \cos(n\theta) \sum_{\alpha} e^{-k\alpha^2(t-t_1)} \frac{\alpha^2 J_n(\alpha r)}{(\alpha^2 - n^2/a^2) J_n(\alpha a)} \right] dt_1, \end{aligned} \quad (15)$$

where τ is the time required to disperse the entire dust bed.

In addition to regression of the leading edge, the dust may be lifted continuously from the entire bed surface. This occurrence is equivalent to a surface source extending from $-\theta_0$ to θ_0 in θ and from 0 to L in z . The expression for this case is obtained by integrating equation 10 with respect

to z_1 from 0 to L . The result is

$$c = \frac{(2\theta_0 QL)}{2\pi^{1/2} a^2 L} \left[\operatorname{erf} \left\{ \frac{z-U(t-t_1)}{2\sqrt{k(t-t_1)}} \right\} - \operatorname{erf} \left\{ \frac{(z-L)-U(t-t_1)}{2\sqrt{k(t-t_1)}} \right\} \right] \cdot \left[1 + \sum_{n=-\infty}^{\infty} \frac{1}{n\theta_0} \sin(n\theta_0) \cos(n\theta) \sum_{\alpha} e^{-k\alpha^2(t-t_1)} \frac{\alpha^2 J_n(\alpha r)}{(\alpha^2 - n^2/a^2) J_n(\alpha a)} \right], \quad (16)$$

where $(2\theta_0 QL)$ is the quantity of mass released instantaneously from the bed surface at $t = t_1$, and

$$\operatorname{erf}(x) = \frac{2}{\sqrt{\pi}} \int_0^x e^{-\zeta^2} d\zeta$$

is the error function. If the dust on the bed surface is released continuously at the rate of $\phi(t_1)$ per unit time, the resulting concentration $c(r, \theta, z, t)$ for $t \geq t_d$ can be obtained by replacing $(2\theta_0 QL)$ in equation 16 by $\phi(t_1) dt_1$ and integrating with respect to t_1 :

$$c = \frac{1}{2\pi^{1/2} a^2 L} \int_0^{t_d} \phi(t_1) \left[\operatorname{erf} \left\{ \frac{z-U(t-t_1)}{2\sqrt{k(t-t_1)}} \right\} - \operatorname{erf} \left\{ \frac{(z-L)-U(t-t_1)}{2\sqrt{k(t-t_1)}} \right\} \right] \cdot \left[1 + \sum_{n=-\infty}^{\infty} \frac{1}{n\theta_0} \sin(n\theta_0) \cos(n\theta) \sum_{\alpha} e^{-k\alpha^2(t-t_1)} \frac{\alpha^2 J_n(\alpha r)}{(\alpha^2 - n^2/a^2) J_n(\alpha a)} \right] dt_1, \quad (17)$$

where t_d is the time at which the dust lifting process is completed. For the case $t < t_d$, t_d should be replaced by t in equation 17. The form of $\phi(t_1)$ may be obtained from experiments.

The Case of Rectangular Cross Sections

Since most mine roadways are rectangular in cross sections (fig. 2), this case is of greater practical interest. Only the system of constant convective velocity U and constant diffusion coefficient k will be considered. The governing equation is

$$\frac{\partial c}{\partial t} + U \frac{\partial c}{\partial z} = k \left(\frac{\partial^2 c}{\partial x^2} + \frac{\partial^2 c}{\partial y^2} + \frac{\partial^2 c}{\partial z^2} \right), \quad (18)$$

and the boundary conditions are

$$\frac{\partial c}{\partial x} = 0 \text{ and } \frac{\partial c}{\partial y} = 0 \text{ at the walls.} \quad (19)$$

The expression for an instantaneous point source of strength Q in the plane $z = z_1$ at the point (x_1, y_1) emitted at time $t = t_1$, is partially derived from

the Jordan report listed in footnote 8 as follows:¹⁰

$$c = \frac{Qe^{-\{(z-z_1)-U(t-t_1)\}^2/4k(t-t_1)}}{2ab\{\pi k(t-t_1)\}^{1/2}} \left\{ 1 + 2 \sum_{n=1}^{\infty} e^{-kn^2\pi^2(t-t_1)/a^2} \cos \frac{n\pi x}{a} \cos \frac{n\pi x_1}{a} \right\} \left\{ 1 + 2 \sum_{n=1}^{\infty} e^{-kn^2\pi^2(t-t_1)/b^2} \cos \frac{n\pi y}{b} \cos \frac{n\pi y_1}{b} \right\}. \quad (20)$$

The expression for an instantaneous line source in the plane $z = z_1$, along $x = x_1$, and $Y_a \leq y \leq Y_b$ can be obtained by integrating equation 20 with respect to y_1 from Y_a to Y_b , giving

$$c = \frac{Q(Y_b - Y_a)e^{-\{(z-z_1)-U(t-t_1)\}^2/4k(t-t_1)}}{2ab\sqrt{\pi k(t-t_1)}} \left[1 + 2 \sum_{n=1}^{\infty} e^{-kn^2\pi^2(t-t_1)/a^2} \cos \frac{n\pi x}{a} \cos \frac{n\pi x_1}{a} \right] \left[1 + \sum_{n=1}^{\infty} \frac{2b}{n\pi(Y_b - Y_a)} e^{-kn^2\pi^2(t-t_1)/b^2} \left\{ \sin \frac{n\pi Y_b}{b} - \sin \frac{n\pi Y_a}{b} \right\} \cos \frac{n\pi y}{b} \right]. \quad (21)$$

For the special case of a line source along $x = 0$, $0 \leq y \leq b$,

$$c = \frac{Qbe^{-\{(z-z_1)-U(t-t_1)\}^2/4k(t-t_1)}}{2ab\sqrt{\pi k(t-t_1)}} \left\{ 1 + 2 \sum_{n=1}^{\infty} e^{-kn^2\pi^2(t-t_1)/a^2} \cos \frac{n\pi x}{a} \right\}. \quad (21-a)$$

It is noted that the dependence on y is absent in equation 21-a, indicating a two-dimensional characteristic of concentration distribution.

If the line source at $z = z_1$ moves according to the relation

$$z_1 = Mt_1^N, \quad (22)$$

the moving velocity of the source is

$$\frac{dz_1}{dt_1} = MNt_1^{N-1}. \quad (23)$$

¹⁰It appears that Jordan's equation 3.2.4 (footnote 8) is not correct when $m = 0$ or $n = 0$; the expression in equation 20 is adopted. The last part of this expression agrees with the Green's function for the rectangular configurations given in equation 14.4(4) of footnote 7.

The source term $Q(Y_b - Y_a)$ in equation 21 is now a function of time,

$$\begin{aligned} Q(Y_b - Y_a) &= Q_1(t_1) dt_1 = \rho(Y_b - Y_a) h \frac{dz_1}{dt_1} \\ &= \rho(Y_b - Y_a) hMN t_1^{N-1} dt_1. \end{aligned} \quad (24)$$

Substituting equation 24 into equation 21 and integrating with respect to t_1 , we obtain for the case of $t < \tau$,

$$\begin{aligned} c &= \frac{\rho(Y_b - Y_a) hMN}{2ab\sqrt{\pi k}} \int_0^t \frac{t_1^{N-1} e^{-\{(z-z_1)-U(t-t_1)\}^2/4k(t-t_1)}}{(t-t_1)^{1/2}} \\ &\quad \left[1 + 2 \sum_{m=1}^{\infty} e^{-kn^2\pi^2(t-t_1)/a^2} \cos \frac{m\pi x}{a} \cos \frac{m\pi x_1}{a} \right] \\ &\quad \left[1 + \sum_{n=1}^{\infty} \frac{2b}{n\pi(Y_b - Y_a)} e^{-kn^2\pi^2(t-t_1)/b^2} \left\{ \sin \frac{n\pi Y_b}{b} - \sin \frac{n\pi Y_a}{b} \right\} \cos \frac{n\pi y}{b} \right] dt_1, \end{aligned} \quad (25)$$

and for the case of $t \geq \tau$,

$$\begin{aligned} c &= \frac{\rho(Y_b - Y_a) hMN}{2ab\sqrt{\pi k}} \int_0^{\tau} \frac{t_1^{N-1} e^{-\{(z-z_1)-U(t-t_1)\}^2/4k(t-t_1)}}{(t-t_1)^{1/2}} \\ &\quad \left[1 + 2 \sum_{m=1}^{\infty} e^{-kn^2\pi^2(t-t_1)/a^2} \cos \frac{m\pi x}{z} \cos \frac{m\pi x_1}{a} \right] \\ &\quad \left[1 + \sum_{n=1}^{\infty} \frac{2b}{n\pi(Y_b - Y_a)} e^{-kn^2\pi^2(t-t_1)/b^2} \left\{ \sin \frac{n\pi Y_b}{b} - \sin \frac{n\pi Y_a}{b} \right\} \cos \frac{n\pi y}{b} \right] dt_1, \end{aligned} \quad (26)$$

where τ is the time for dispersing the entire dust pile.

Next consider an instantaneous plane source along the bottom surface of the dust $x = 0$, $Y_a \leq y \leq Y_b$, and extending from $z = 0$ to $z = L$. The expression for this case is obtained by integrating equation 21 with respect to z_1 from 0 to L . The result is similar to the case for a circular cross section.

$$\begin{aligned} c &= \frac{Q(Y_b - Y_a)L}{2abL} \left[\operatorname{erf} \left\{ \frac{z-U(t-t_1)}{2\sqrt{k(t-t_1)}} \right\} - \operatorname{erf} \left\{ \frac{(z-L)-U(t-t_1)}{2\sqrt{k(t-t_1)}} \right\} \right] \\ &\quad \left[1 + 2 \sum_{m=1}^{\infty} e^{-kn^2\pi^2(t-t_1)/a^2} \cos \frac{m\pi x}{a} \cos \frac{m\pi x_1}{a} \right] \left[1 + \sum_{n=1}^{\infty} \frac{2b}{n\pi(Y_b - Y_a)} \right. \\ &\quad \left. e^{-kn^2\pi^2(t-t_1)/b^2} \left\{ \sin \frac{n\pi Y_b}{b} - \sin \frac{n\pi Y_a}{b} \right\} \cos \frac{n\pi y}{b} \right], \end{aligned} \quad (27)$$

where $Q(Y_b - Y_a)L$ is the quantity of mass liberated instantaneously on the plane. If the plane source liberates dust continuously at the rate $\phi(t_1)$ per unit time from $t_1 = 0$ to $t_1 = t_d$, then

$$Q(Y_b - Y_a)L = \phi(t_1) dt_1, \quad (28)$$

and the concentration $c(x, y, z, t)$ for $t \geq t_d$ is

$$c = \frac{1}{2abL} \int_0^{t_d} \phi(t_1) \left[\operatorname{erf} \left\{ \frac{z-U(t-t_1)}{2\sqrt{k(t-t_1)}} \right\} - \operatorname{erf} \left\{ \frac{(z-L)-U(t-t_1)}{2\sqrt{k(t-t_1)}} \right\} \right] \cdot \\ \left[1 + 2 \sum_{m=1}^{\infty} e^{-km^2 \pi^2 (t-t_1)/a^2} \cos \frac{m\pi x}{a} \cos \frac{m\pi x_1}{a} \right] \left[1 + \sum_{n=1}^{\infty} \frac{2b}{n\pi(Y_b - Y_a)} \cdot \right. \\ \left. e^{-kn^2 \pi^2 (t-t_1)/b^2} \left\{ \sin \frac{n\pi Y_b}{b} - \sin \frac{n\pi Y_a}{b} \right\} \cos \frac{n\pi y}{b} \right] dt_1.$$

The functional relation $\phi(t_1)$ may be obtained from experiments. If the source releases dust at a constant rate Q_s from $t = t_1$ to t_d then for $t \geq t_d$

$$c = \frac{Q_s}{2abL} \int_0^{t_d} \left[\operatorname{erf} \left\{ \frac{z-U(t-t_1)}{2\sqrt{k(t-t_1)}} \right\} - \operatorname{erf} \left\{ \frac{(z-L)-U(t-t_1)}{2\sqrt{k(t-t_1)}} \right\} \right] \cdot \\ \left[1 + 2 \sum_{m=1}^{\infty} e^{-km^2 \pi^2 (t-t_1)/a^2} \cos \frac{m\pi x}{a} \cos \frac{m\pi x_1}{a} \right] \left[1 + \sum_{n=0}^{\infty} \frac{2b}{n\pi(Y_b - Y_a)} \cdot \right. \\ \left. e^{-kn^2 \pi^2 (t-t_1)/b^2} \left\{ \sin \frac{n\pi Y_b}{b} - \sin \frac{n\pi Y_a}{b} \right\} \cos \frac{n\pi y}{b} \right] dt_1.$$

RESULTS

Experimental Data Used in Computations

The following data based on rock dust dispersal in a 0.6-m-diameter, 50-m-long explosion duct will be used in the computation. (See footnote 9.) The dust bed regresses as a line source from the leading edge, being entrained with increasing speed by a velocity pulse that increases from 0 to 6,000 cm/sec in 0.318 sec. In this case

$L = 20.4$ -cm length of bed,

$2a\theta_0 = 5.1$ -cm width of bed,

$h = 1.25$ -cm height of bed,

$a = 30$ -cm radius of explosion tunnel,

and total mass of dust bed = 138 g.

The mass bulk density of the bed is calculated as

$$\rho = \frac{138}{(20.4)(5.1)(1.25)} = 1.06 \text{ gm/cm}^3. \quad (31)$$

Next, the constants M and N in equation 11 or 22 will be determined. By fitting the data points in figure 5 at $z_1 = 5.1$ cm and 20.4 cm, two simultaneous equations for M and N are obtained:

$$5.1 = M(0.244)^N,$$

and

$$20.4 = M(0.318)^N.$$

The values of M and N are determined as

$$M = 8160,$$

$$N = 5.23,$$

thus,
$$z_1 = 8160 (t_1)^{5.23}. \quad (32)$$

The agreement between this two-parameter equation and the experimental points is satisfactory, as can be seen in figure 5. The entrainment of coal dust by the velocity pulse follows the same general relationship.

Data for computing the diffusion coefficient k for the present situation are not available. An estimate can be made, however. Soo and coworkers¹¹ give the following values of k obtained in a 1.27-cm-diameter tube:

	Concentration, mg/lit	k, cm ² /sec
Glass particles.....50 μ m (nominal)..	4.80	7.96
	7.81	10.3
Mg particles.....35 μ m (nominal)..	0.239	1.15
	0.530	1.59
	0.842	1.88
Glass.....100-250 μ m (nominal)..	-	2.7
Catalyst.....20-150 μ m (nominal)..	15.5	8
	26.5	9.45
	70	13

Soo and Trezek¹² give wall diffusivities of magnesia particles in air as functions of particle loading ratio and flow velocities. For a mass ratio of solid to gas of 1.0,

$$k = 1.4 \text{ cm}^2/\text{sec} \text{ for flow velocity} = 42.7 \text{ m/sec},$$

and
$$k = 0.19 \text{ cm}^2/\text{sec} \text{ for flow velocity} = 18.9 \text{ m/sec}.$$

Taylor¹³ gives the radial diffusion coefficient for soluble material in a fluid in turbulent flow as

$$k = 0.052 aU/\overline{F/2}, \quad (33)$$

¹¹Soo, S. L., G. J. Trezek, R. C. Dunick, and G. F. Hohnstreiter. Concentration and Mass Flow Distributions in a Gas-Solid Suspension. I&EC Fundamentals, v. 3, 1964, p. 98.

¹²Soo, S. L., and G. J. Trezek. Turbulent Pipe Flow of Magnesia Particles in Air. I&EC Fundamentals, v. 5, 1966, p. 388.

¹³Taylor, G. I. The Dispersion of Matter in Turbulent Flow Through a Pipe. Proc. Roy. Soc. (London), Ser. A, v. 223, 1954, pp. 446-468.

where a , U , and f are the channel radius, mean stream velocity, and Fanning friction factor, respectively. The friction factor f is 0.003 from the Moody diagram, using $U = 6000$ cm/sec, $a = 30$ cm, $\nu = 20.9 \times 10^{-2}$ cm²/sec, and $Re = 2aU/\nu = 1.72 \times 10^6$. Hence,

$$\begin{aligned} k &= 0.052(30)(6000)\sqrt{0.003/2} \\ &= 362 \text{ cm}^2/\text{sec}. \end{aligned}$$

This value of k is an upper bound for the dust-air system since the diffusion coefficient of dust cannot be greater than the diffusion coefficient of soluble material in the same fluid.

Calculated eddy diffusivities ϵ in the core of a turbulent airstream flowing at 60 m/sec in a 53.2-cm-square duct are in the range of 5 to 500 cm²/sec, based on the equation of Martinelli,¹⁴

$$\epsilon = [U_* (1-x/r_0)x/2.5] - \nu,$$

where the friction velocity is $U_* = U(f/2)^{0.5}$, x is the vertical distance from the wall, and ν is the kinematic viscosity. For $3 < Re < 3 \times 10^6$, the friction factor $f = 0.00140 + 0.125 (Re)^{-0.32}$.

It has been noted^{15 16} that dust particles leave the bed with a lateral velocity estimated by Owen¹⁷ to be of the order of the friction velocity of the gas. This mode of particle transport cannot be included in the present theory. However, the effect of initial particle velocity will be to increase the rate of lateral particle transport, the effective value of k .

A "best" k value for the present calculation appears to be within the range of 25 to 100 cm²/sec, based on the previous discussion. Any values of k can be accommodated in the computer program that solves the working equations.

¹⁴Martinelli, R. C. Heat Transfer and Molten Metals. Trans. ASME, v. 29, November 1946, pp. 947-955.

¹⁵Owen, P. R. Saltation of Uniform Grains in Air. J. Fluid Mech., v. 20, 1964, p. 225.

¹⁶Works cited in footnote 4.

¹⁷Work cited in footnote 15.

Results of Computations and Discussion

Figures 6 to 9 show calculated concentration distributions in a square channel ($a = b = 53.2$ cm) at times 0.1, 0.2, 0.3, and 1.0 sec after initiation of dust dispersion, with $U_{\text{ave}} = 500$ cm/sec and $k = 50$ cm²/sec. The bed covers the entire bottom width of the channel base with an axial length $L = 20.4$ cm. The location of the regressing leading edge of the bed is given by equation 32.

The dust cloud is confined to the lower part of the channel and moves in the downstream direction. The dust concentration is maximum at the dust bed and diminishes as the normal distance from the bed increases. As time progresses, the dust cloud is convected with a velocity U and diffuses in both axial and lateral direction.

It may be noted that in our experimental tunnel, a velocity reversal occurs at $t \approx 0.6$ sec because of pressure wave interaction in the explosion

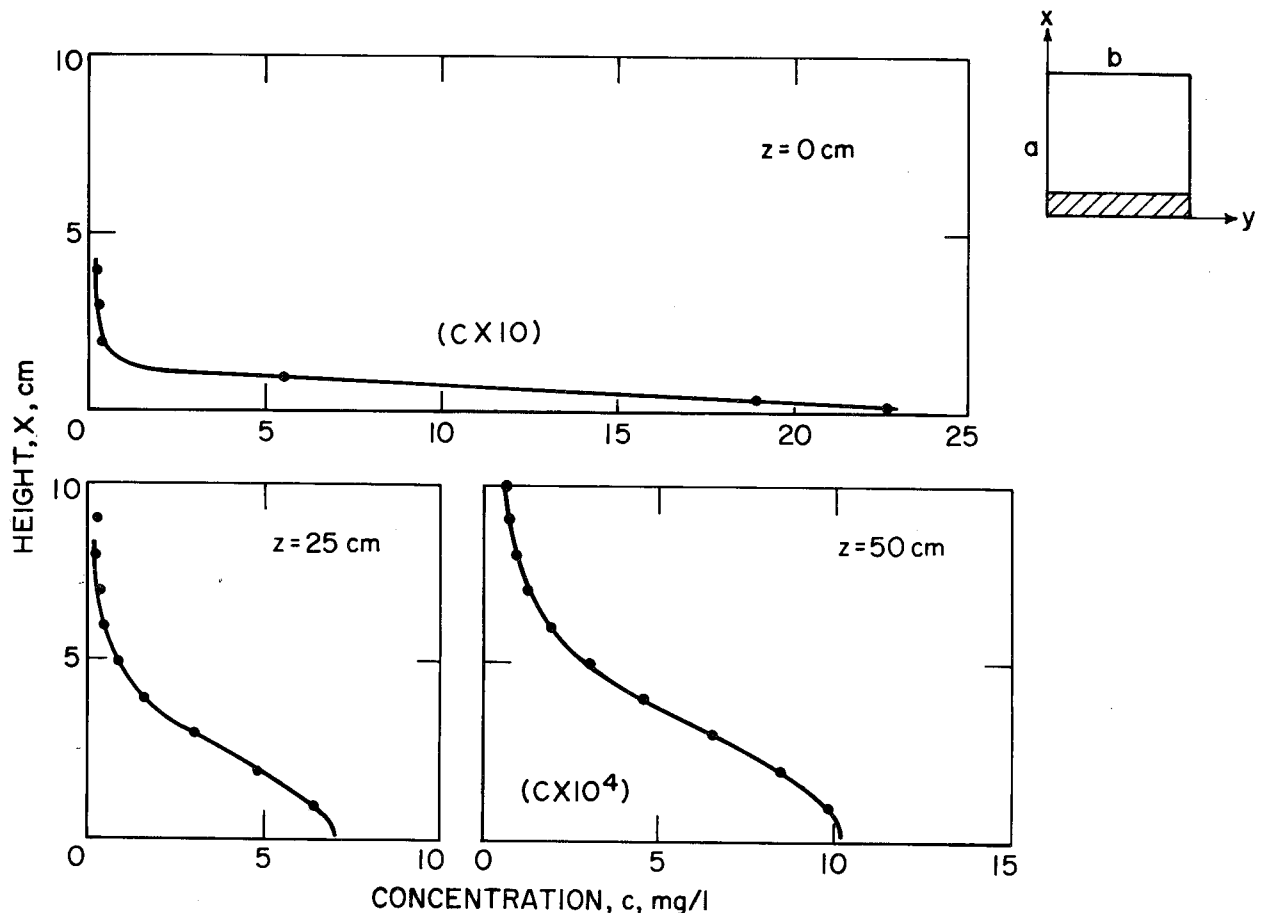


FIGURE 6. - Dust concentration as a function of distance from wall in a square channel at $t = 0.1$ sec ($a = b = 53.2$ cm, $U = 5$ m/sec, $k = 50$ cm²/sec, total dust mass = 140 gm).

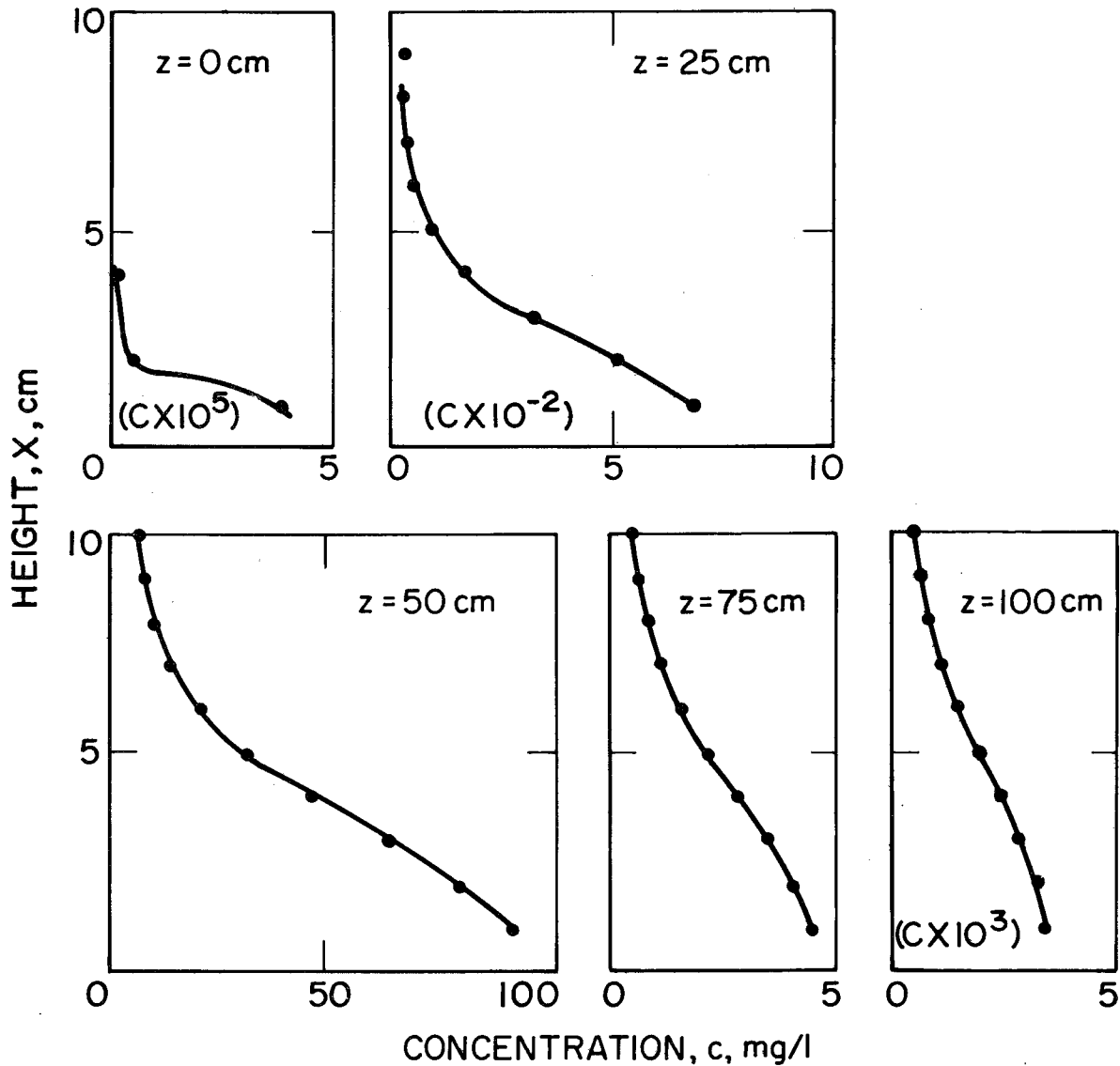


FIGURE 7. - Dust concentration in a square channel at $t = 0.2$ sec ($a = b = 53.2$ cm, $U = 50$ m/sec, $k = 50$ cm²/sec, total dust mass = 140 gm).

process. The present calculations assume steady flow instead of the pulsed velocity actually induced by the explosion. The effect of gravity has also been neglected. This omission may be partially justified since gravitational settling should be relatively unimportant in the early stage of dispersion, to which the analysis applied. Cases for which U varies in the direction

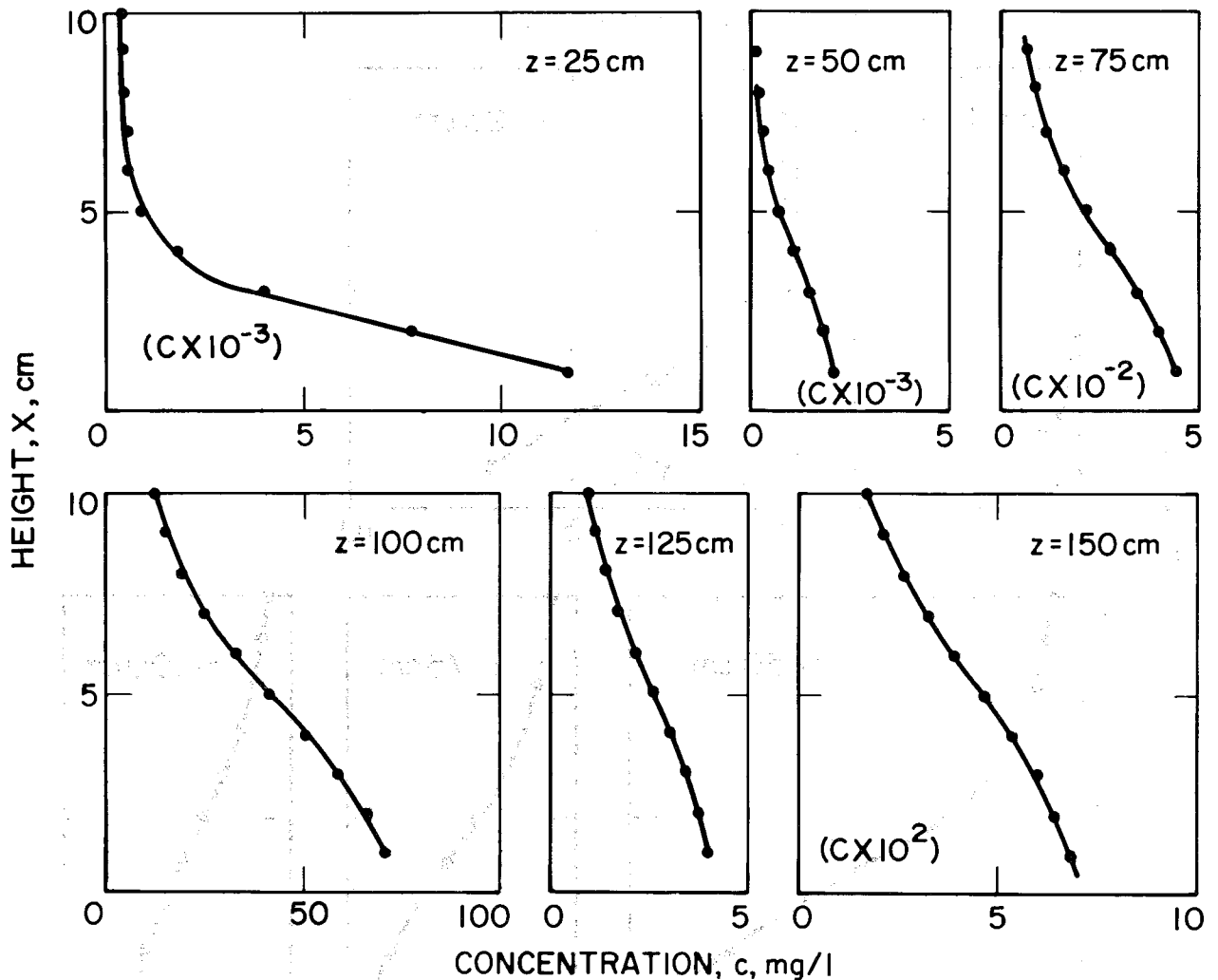


FIGURE 8. - Dust concentration in a square channel at $t = 0.3$ sec ($a = b = 53.2$ cm, $U = 5$ m/sec, $k = 50$ cm²/sec, total dust mass = 140 gm).

perpendicular to the flow from axial locations have been considered.¹⁸ To include the effects of variable U and gravity, it is more convenient to reformulate the governing equations¹⁹ and solve them by means of a numerical technique.

¹⁸Aris, R. On the Dispersion of a Solute in a Fluid Flowing Through a Tube. Proc. Roy Soc. A., v. 235, 1956, pp. 67-78.

Atesmen, K. M. The Dispersion of Matter in Turbulent Shear Flow. Int. J. Heat Mass Transfer, v. 14, 1971, pp. 2146-2152.

¹⁹Soo, S. L. Ch. in Fluid Dynamics of Multiphase Systems, Blaisdell Publishing Company, Waltham, Mass., 1967, pp. 248-276.

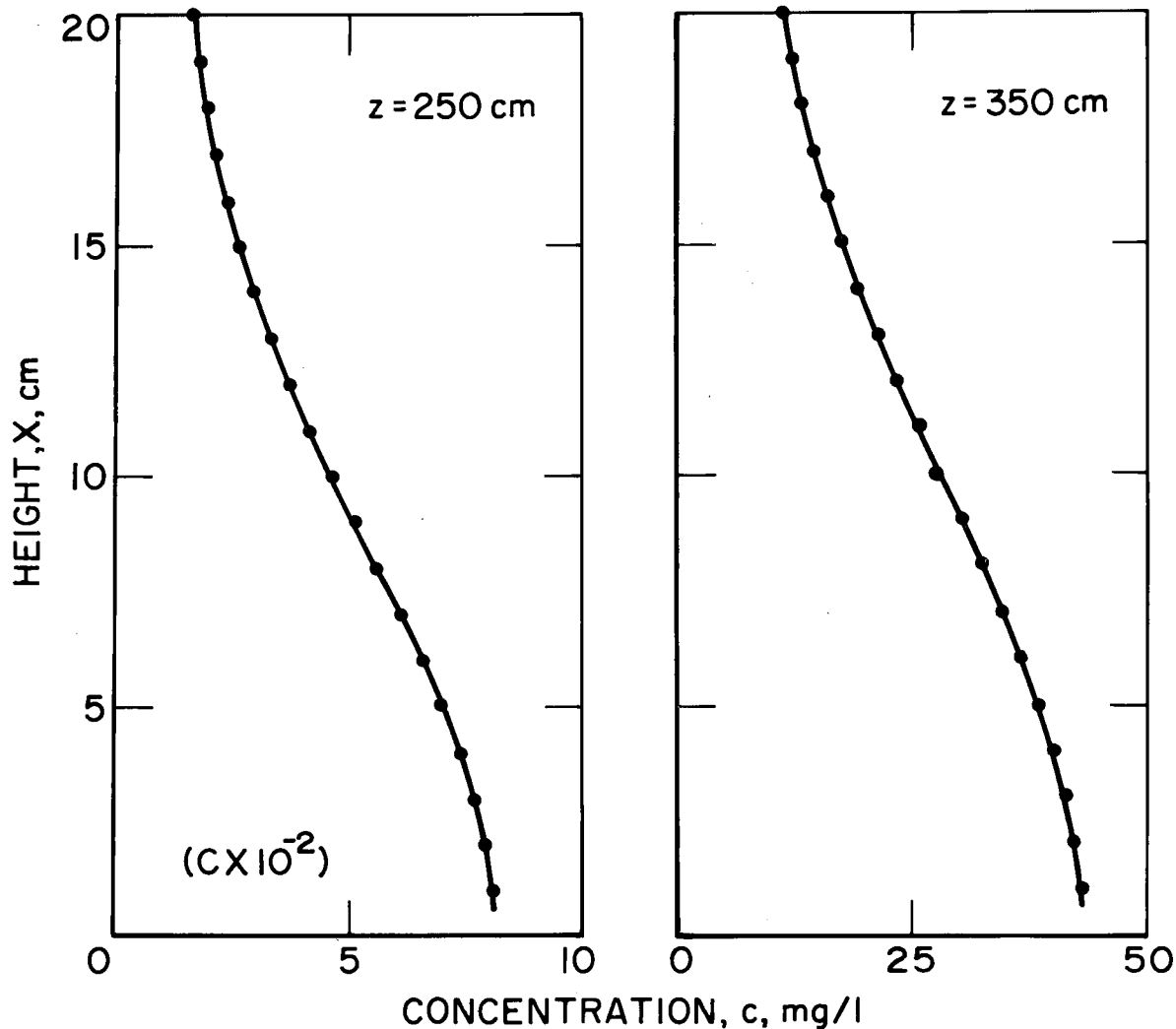


FIGURE 9. - Dust concentration in a square channel at $t = 1.0$ sec ($a = b = 53.2$ cm, $U = 5$ m/sec, $k = 50$ cm²/sec, total dust mass = 140 gm).

When a dust pile extends over only a central portion of the channel floor ($Y_a = 24.05$ cm and $Y_b = 29.15$ cm in equation 26), diffusion takes place in the y direction as well as in the x direction. Figures 10 and 11 show the vertical dust concentration distributions along the z axis at $y = 26.6$ cm (center) and $y = 13.3$ cm (halfway between the center and side wall) 0.1 and 0.3 sec after initiation of dispersion with $U = 5$ m/sec and $k = 50$ cm²/sec. Diffusion in the y direction yields dust concentrations that are viable but always less than at the center. Figures 10 and 11 also show results of a computation for a circular channel of radius = 30 cm based on equation 16 for the same flow and diffusivity. Concentrations under the same conditions in a circular cross section are less near the wall, but higher at larger distances.

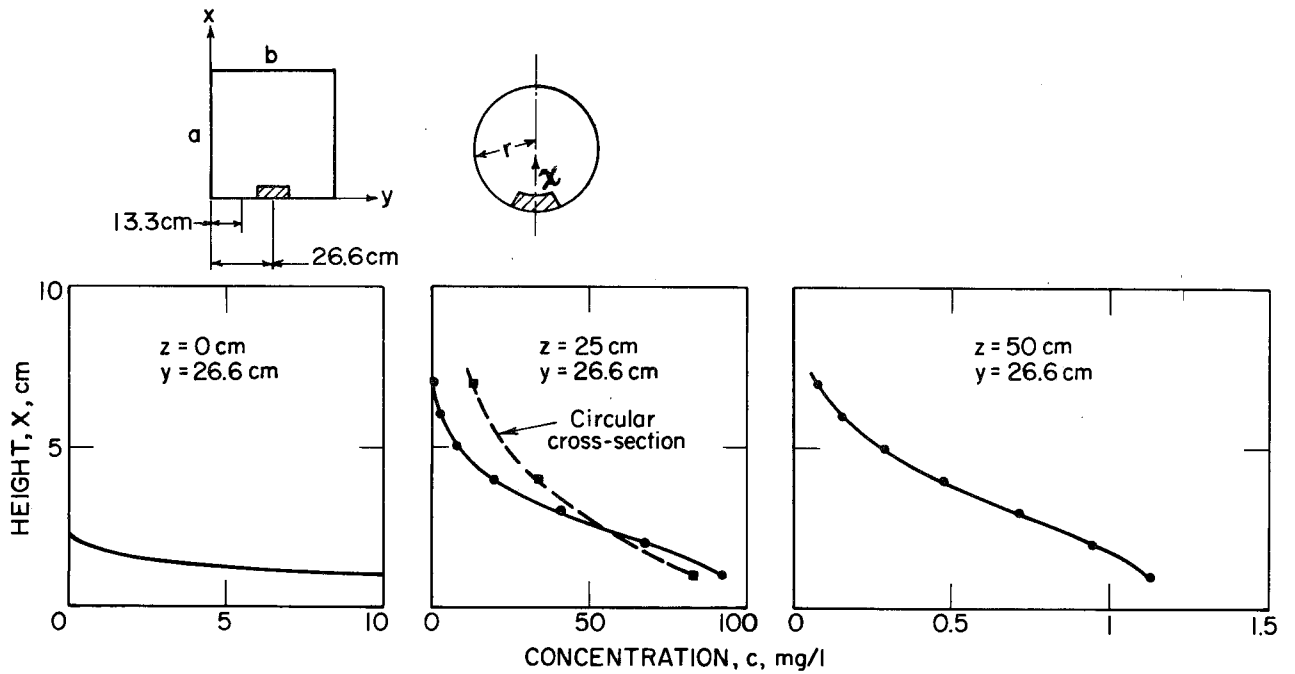


FIGURE 10. - Dust concentration in a square and a circular channel as a function of distance from wall at $t = 0.1$ sec ($a = b = 53.2$ cm, $r = 30$ cm, $U = 5$ m/sec, $k = 50$ cm²/sec, total dust mass = 140 gm).

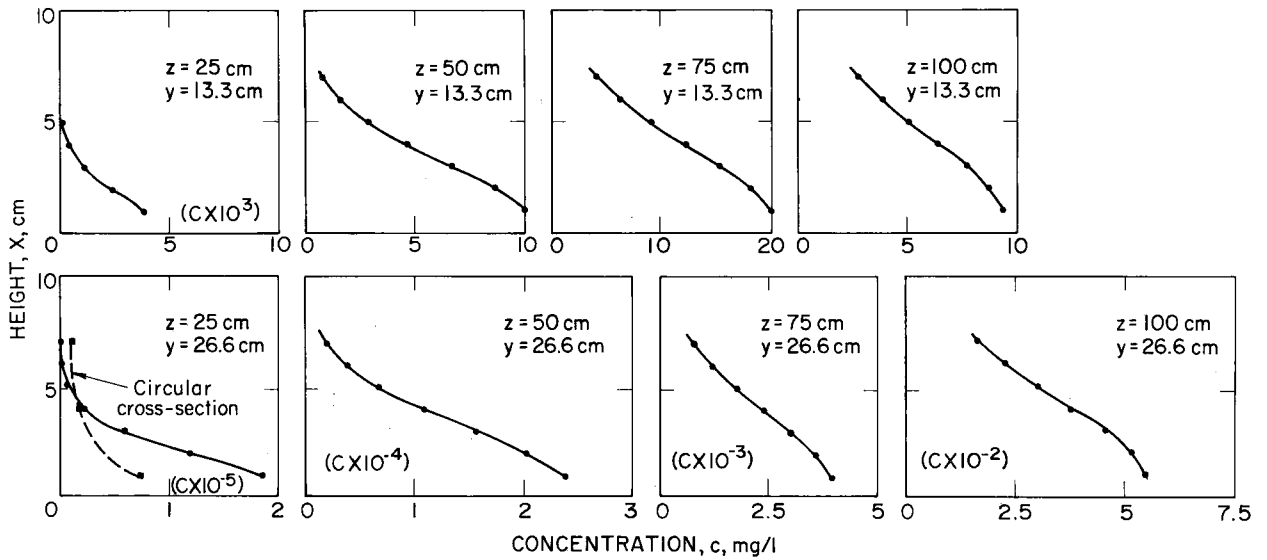


FIGURE 11. - Dust concentration in a square and a circular channel as a function of distance from wall at $t = 0.3$ sec ($a = b = 53.2$ cm, $r = 30$ cm, $U = 5$ m/sec, $k = 50$ cm²/sec, total dust mass = 140 gm).

The effect of increasing k from 25 to 100 cm^2/sec is shown in table 1 for the same centrally located dust bed in the 53.2 cm^2 duct. Table 2 shows the effect of changing the average flow velocity from 5 to 50 m/sec . Higher values of k are seen to give faster dust spreading after dispersion has been initiated, and higher concentrations. The effect of higher velocity is to dilute the concentrations more rapidly after entrainment.

Since the diffusion equation 1 is linear, the solutions derived in the Analysis section of this report may be superimposed to give dust concentrations due to a combination of sources (stationary and moving). For instance, these formulas can be applied to the case in which dust is removed from the ceiling as well as from the floor of a channel. For the case of mixed coal dust and rock dust in one pile, the concentrations in the stream for each particle type may be obtained by applying the formula twice, once using k_1 for coal dust, and once using k_2 for rock dust. Since rock dust is heavier than coal dust, at the initial stage of dispersion the values of U for coal dust and rock dust are also different owing to a difference in their response to the fluid drags. However, this difference was found to be small in the explosion tunnel experiments and may be neglected. It should be noted that initially ($t = 0$) the dust concentration is zero for all cases. Table 3 compares dust concentrations in space and time when entrainment occurs by surface lifting or as a regressing line source. The faster surface-lifting mode of dispersion results in more rapid initial spreading of the dust cloud, and then faster dilution by the airstream to lower concentrations.

Three additional examples of dust dispersion that can be solved by the present additive treatment follow. In the first, consider a square duct with $a = b = 53.2$ cm ; the roof and two sides are covered with a 0.32 cm coal dust layer, while the floor holds a 1.25 cm thick layer of rock dust. All beds are 20.3 cm long. Entrainment by regression from the leading edge is initiated simultaneously for the two layers. Entrainment rates of coal and rock dust follow equations 25 and 26 with $U_{ave} = 50$ m/sec and $k = 100$ cm^2/sec for the coal and rock dust. The juxtaposed coal and rock dust concentrations in the airborne mixtures are given at several central downstream locations in table 4, at 0.1, 0.2, 0.3, and 0.5 sec . Bulk densities of coal and rock dust are 0.693 and 1.06 gm/cc , respectively. In this and the following examples, z is taken to be the same for coal and rock dust. The dust concentrations in the central area of the dust reach maximum at 1600 cm distance ($t = 0.5$ sec). Apparently normal dilution by the airstream is overcome as the dust spreads to this location from all sides during the available time period.

TABLE 1. - The effect of the diffusion coefficient, k , on rock dust concentration

(Height of dust bed = 1.25 cm, $U = 500$ cm/sec, $k = 25$ and 100 cm²/sec, duct height and width = 53.2 cm; dust concentration in mg/liter)

z , cm	0.1 sec		0.2 sec		0.3 sec		0.5 sec		1.0 sec	
	$k = 25$	$k = 100$	$k = 25$	$k = 100$	$k = 25$	$k = 100$	$k = 25$	$k = 100$	$k = 25$	$k = 100$
$x = 0$										
25	170	580	1.8×10^4	5.9×10^3	3.7×10^5	1.3×10^5	0	0	0	0
50	0	2.4×10^{-2}	1.8×10^3	550	4.3×10^4	1.3×10^4	0	0	0	0
100	0	0	1.2×10^{-2}	5.8×10^{-2}	1.0×10^3	300	35	2.6×10^3	0	0
200	0	0	0	0	0	0	550	1.7×10^3	0	0
400	0	0	0	0	0	0	0	0	6.3×10^3	1.9×10^3
800	0	0	0	0	0	0	0	0	8.3×10^{-10}	4.6×10^{-13}
1600	0	0	0	0	0	0	0	0	0	0
$x = 10$ cm										
25	4.9×10^{-7}	0.32	5.5×10^{-5}	37	7.1×10^{-8}	130	0	0	0	0
50	0	1.2×10^{-3}	8.3×10^{-2}	42	8.8×10^2	880	0	0	0	0
100	0	0	5.8×10^{-5}	1.4×10^{-2}	82	82	0.16	710	0	0
200	0	0	0	0	0	0	44	87	0	0
400	0	0	0	0	0	0	0	0	1.8×10^3	1.4×10^3
800	0	0	0	0	0	0	0	0	6.8×10^{-11}	0
1600	0	0	0	0	0	0	0	0	0	0
$x = 20$ cm										
25	8.4×10^{-12}	3.2×10^{-7}	7.2×10^{-8}	6.4×10^{-5}	1.6×10^{-5}	4.6×10^{-5}	0	0	0	0
50	0	1.7×10^{-7}	1.7×10^{-9}	2.4×10^{-2}	1.2×10^{-6}	0.45	0	0	0	0
100	0	0	6.7×10^{-12}	2.0×10^{-4}	3.4×10^{-6}	1.8	1.8×10^{-3}	15	0	0
200	0	0	0	0	0	0	2.3×10^{-2}	13	0	0
400	0	0	0	0	0	0	0	0	40	530
800	0	0	0	0	0	0	0	0	0	0
1600	0	0	0	0	0	0	0	0	3.8×10^{-14}	0

TABLE 2. - The effect of velocity on rock dust concentration

(Height of dust bed = 1.25 cm, k = 100 cm²/sec, U = 5 and 50 m/sec, duct height and width = 53.2 cm; dust concentration in mg/liter)

z \ t, cm	0.1 sec		0.2 sec		0.3 sec		0.5 sec		1.0 sec	
	U = 5	U = 50	U = 5	U = 50	U = 5	U = 50	U = 5	U = 50	U = 5	U = 50
x = 0										
25	580	430	5.9X10 ⁴	9.5X13 ⁸	1.3X10 ⁵	8.8X10 ⁴	0	0	0	0
50	2.4X10 ⁻²	230	550	5.5X10 ³	1.3X10 ⁴	4.2X10 ⁴	0	0	0	0
100	0	83.8	5.8X10 ⁻²	2.6X10 ³	300	2.0X10 ⁴	2.6X10 ³	0	0	0
200	0	13.9	0	890	0	7.5X10 ³	1.7X10 ³	0	0	0
400	0	7.2X10 ⁻²	0	140	0	1.9X10 ³	0	0	1.9X10 ³	0
800	0	0	0	0.69	0	140	0	0	4.6X10 ⁻¹³	0
1600	0	0	0	0	0	0	0	190	0	0
x = 10 cm										
25	0.32	6.1X10 ⁻¹⁰	37	1.1X10 ⁻⁸	1.3X10 ²	4.4X10 ⁻⁸	0	0	0	0
50	1.2X10 ⁻³	3.4X10 ⁻⁹	42	2.9X10 ⁻⁸	880	5.7X10 ⁻⁸	0	0	0	0
100	0	3.2X10 ⁻⁴	1.4X10 ⁻²	8.8X10 ⁻³	82	1.7X10 ⁻²	710	0	0	0
200	0	2.7X10 ⁻²	0	1.7	0	11	87	0	0	0
400	0	3.1X10 ⁻³	0	6.1X10 ⁻²	0	80	0	0	1.4X10 ³	0
800	0	0	0	0.15	0	29	0	0	0	0
1600	0	0	0	0	0	0	0	86	0	0
x = 20 cm										
25	3.2X10 ⁻⁷	1.1X10 ⁻¹⁰	6.4X10 ⁻⁵	3.3X10 ⁻⁹	4.6X10 ⁻⁵	7.3X10 ⁻⁸	0	0	0	0
50	1.7X10 ⁻⁷	1.9X10 ⁻¹⁰	2.4X10 ⁻²	2.7X10 ⁻⁹	0.45	9.4X10 ⁻¹⁰	0	0	0	0
100	0	1.2X10 ⁻¹⁰	2.0X10 ⁻⁴	2.4X10 ⁻⁹	1.8	4.7X10 ⁻⁹	15	0	0	0
200	0	1.7X10 ⁻¹⁰	0	9.9X10 ⁻⁹	0	3.0X10 ⁻⁸	13	0	0	0
400	0	2.6X10 ⁻⁷	0	5.2X10 ⁻⁴	0	6.4X10 ⁻³	0	0	530	0
800	0	0	0	1.3X10 ⁻³	0	0.27	0	0	0	0
1600	0	0	0	0	0	0	0	8.2	0	0

TABLE 3. - Surface lifting versus line source lifting of rock dust

(Height of dust bed = 1.25 cm, $k = 100 \text{ cm}^2/\text{sec}$,
 $U = 50 \text{ m/sec}$, duct height and width = 53.2 cm;
dust concentration in mg/liter)

z\ t, cm	0.1 sec		0.2 sec		0.3 sec		0.5 sec		1.0 sec	
	Surface	Line source	Surface	Line source	Surface	Line source	Surface	Line source	Surface	Line source
$x = 0$										
25	450	430	1.3×10^{-8}	9.5×10^3	670	8.8×10^4	0	0	0	0
50	520	230	520	5.5×10^3	1.5×10^3	4.2×10^4	0	0	0	0
100	220	83.8	450	2.6×10^3	670	2.0×10^4	0	0	0	0
200	75	13.9	140	890	210	7.5×10^3	0	0	0	0
400	29	7.2×10^{-2}	29	140	42	1.9×10^3	0	0	0	0
800	0	0	12	0.69	5.8	140	0	0	0	0
1600	0	0	0	0	0	0	7.5	190	0	0
$x = 10 \text{ cm}$										
25	1.8×10^{-9}	6.1×10^{-10}	0	1.1×10^{-8}	2.7×10^{-9}	4.4×10^{-8}	0	0	0	0
50	2.5×10^{-9}	3.4×10^{-9}	2.5×10^{-9}	2.9×10^{-8}	7.4×10^{-9}	5.7×10^{-8}	0	0	0	0
100	6.8×10^{-4}	3.2×10^{-4}	1.4×10^3	8.8×10^{-3}	2.0×10^3	1.7×10^{-2}	0	0	0	0
200	13	2.7×10^{-2}	24	1.7	36	11	0	0	0	0
400	13	3.1×10^{-3}	1.2	6.1×10^{-2}	1.7	80	0	0	0	0
800	0	0	2.6	0.15	1.2	29	0	0	0	0
1600	0	0	0	0	0	0	3.5	86	0	0
$x = 20 \text{ cm}$										
25	1.1×10^{-9}	1.1×10^{-10}	0	3.3×10^{-9}	1.7×10^{-9}	7.3×10^{-8}	0	0	0	0
50	6.7×10^{-10}	1.9×10^{-10}	6.7×10^{-10}	2.7×10^{-9}	2.0×10^{-9}	9.4×10^{-10}	0	0	0	0
100	5×10^{-10}	1.2×10^{-10}	1×10^{-9}	2.4×10^{-9}	1.5×10^{-9}	4.7×10^{-9}	0	0	0	0
200	4.8×10^{-10}	1.7×10^{-10}	7×10^{-10}	9.9×10^{-9}	1.0×10^{-9}	3.0×10^{-8}	0	0	0	0
400	1×10^{-4}	2.6×10^{-7}	8.9×10^{-3}	5.2×10^{-4}	1.3×10^{-4}	6.4×10^{-3}	0	0	0	0
800	0	0	2.4×10^{-2}	1.3×10^{-3}	1.1×10^{-2}	0.27	0	0	0	0
1600	0	0	0	0	0	0	3.3	8.2	0	0

TABLE 4. - Surface lifting of 0.32-cm coal dust beds from side and roof, and line source lifting of 1.25-cm rock dust beds from floor

($k = 100 \text{ cm}^2/\text{sec}$, $U = 50 \text{ m/sec}$, duct height and width = 53.2 cm, bed length = 20.3 cm; dust concentration in mg/liter)

x, cm	Coal		Rock for y = 20 and 30 cm	x, cm	Coal		Rock for y = 20 and 30 cm
	y = 20 cm	y = 30 cm			y = 20 cm	y = 30 cm	
t = 0.1 sec, z = 25 cm				t = 0.1 sec, z = 400 cm			
20	3.6×10^{-9}	3.6×10^{-9}	1.1×10^{-10}	20	0	0	5.5×10^{-7}
30	1.8×10^{-9}	1.8×10^{-9}	3.0×10^{-11}	30	0	0	4.3×10^{-13}
t = 0.2 sec, z = 25 cm				t = 0.2 sec, z = 400 cm			
20	3.1×10^{-7}	3.1×10^{-7}	3.3×10^{-9}	20	1.9×10^{-3}	1.9×10^{-3}	1.1×10^{-2}
30	2.0×10^{-7}	2.0×10^{-7}	2.3×10^{-9}	30	3.8×10^{-6}	3.8×10^{-6}	8.3×10^{-10}
t = 0.3 sec, z = 25 cm				t = 0.3 sec, z = 400 cm			
20	3.1×10^{-6}	3.1×10^{-6}	4.4×10^{-8}	20	2.3×10^{-3}	2.3×10^{-3}	1.3×10^{-2}
30	1.4×10^{-6}	1.4×10^{-6}	7.3×10^{-8}	30	4.6×10^{-6}	4.6×10^{-6}	1.0×10^{-8}
t = 0.5 sec, z = 25 cm				t = 0.5 sec, z = 400 cm			
20	0	0	0	20	1.9×10^{-18}	1.9×10^{-18}	5.9×10^{-13}
30	0	0	0	30	3.8×10^{-18}	3.8×10^{-18}	5.7×10^{-18}
t = 0.1 sec, z = 50 cm				t = 0.1 sec, z = 800 cm			
20	1.1×10^{-8}	1.1×10^{-8}	2.1×10^{-10}	20	0	0	0
30	1.6×10^{-8}	1.6×10^{-8}	6.0×10^{-11}	30	0	0	0
t = 0.2 sec, z = 50 cm				t = 0.2 sec, z = 800 cm			
20	1.7×10^{-8}	1.7×10^{-8}	2.9×10^{-9}	20	5.9×10^{-4}	5.9×10^{-4}	3.8×10^{-3}
30	4.9×10^{-8}	4.9×10^{-8}	4.9×10^{-10}	30	1.2×10^{-3}	1.2×10^{-3}	1.5×10^{-6}
t = 0.3 sec, z = 50 cm				t = 0.3 sec, z = 800 cm			
20	1.6×10^{-14}	1.6×10^{-14}	1.1×10^{-9}	20	0.13	0.13	0.77
30	2.1×10^{-14}	2.1×10^{-14}	1.2×10^{-9}	30	0.26	0.26	3.1×10^{-4}
t = 0.5 sec, z = 50 cm				t = 0.5 sec, z = 800 cm			
20	0	0	0	20	1.1×10^{-6}	1.1×10^{-6}	4.3×10^{-18}
30	0	0	0	30	2.2×10^{-6}	2.2×10^{-12}	2.2×10^{-21}
t = 0.1 sec, z = 100 cm				t = 0.1 sec, z = 1600 cm			
20	1.1×10^{-8}	1.1×10^{-8}	1.5×10^{-10}	20	0	0	0
30	1.4×10^{-8}	1.4×10^{-8}	5.8×10^{-11}	30	0	0	0
t = 0.2 sec, z = 100 cm				t = 0.2 sec, z = 1600 cm			
20	3.6×10^{-7}	3.6×10^{-7}	3.0×10^{-9}	20	0	0	0
30	4.2×10^{-7}	4.2×10^{-7}	5.8×10^{-10}	30	0	0	0
t = 0.3 sec, z = 100 cm				t = 0.3 sec, z = 1600 cm			
20	3.0×10^{-8}	3.0×10^{-8}	5.5×10^{-9}	20	0	0	0
30	1.3×10^{-6}	1.3×10^{-6}	2.2×10^{-8}	30	0	0	0
t = 0.5 sec, z = 100 cm				t = 0.5 sec, z = 1600 cm			
20	0	0	0	20	4.9	4.9	33
30	0	0	0	30	9.8	9.8	0.66

In the second example, a 0.32-cm layer of coal dust on a 1.25-cm layer of rock dust is located on the floor of a square duct where $a = b = 53.2$ cm; the length of the layered bed is 20.3 cm and the entire width of the floor is covered. The top layer disperses continuously as a surface source (equation 27), and the bottom layer by line source regression (equations 25 and 26). This mode of dispersion, in which a top layer can erode before the bottom layer, is possible when marginal and near-threshold velocities are generated by the explosion. Table 5 shows the separately computed coal and rock dust concentrations in successive time and space coordinates. At locations farther downstream, coal dust concentrations exceed rock dust concentrations despite the initially high proportion of rock to coal dust in the dust bed.

Finally, coal and rock dust concentrations are computed in a typical mine entry cross section, 6 m wide by 4 m high. A 7.62-cm-thick layer of a uniform mixture of 65 percent rock dust and 35 percent coal dust stretches across the width of the floor with length $L = 3$ m, $U = 50$ m/sec, eddy diffusivities $k_{\text{rock dust}} = 50$ cm²/sec, and $k_{\text{coal dust}} = 100$ cm²/sec. The computation is made using these assumed diffusivities to demonstrate the method. Table 6 shows the concentrations for times 0.1, 0.2, 0.3, 0.5, and 1.0 sec after initiation of dust entrainment, based on surface source entrainment (equation 27). Proportions of coal to rock dust larger than unity exist in the dust cloud after 0.3 sec at $x = 10$ cm above the floor, and $z = 25$ cm downstream, owing to the assigned diffusivities.

Mixtures of coal and rock dust containing less than 65 percent rock dust are below recommended safe standards in coal mines. Another factor that contributes to the fire hazard in mines is that, whereas coal dust concentrations below 40 to 50 mg/liter (without rock dust) are nonflammable, very small coal dust concentrations will support methane combustion with an equivalence of about 1 mg/liter coal = 1.6 mg/liter methane at flame ignition conditions.²⁰ The present calculations, which place values of dust concentrations in time and space coordinates, is a first effort that should improve as more experimental data on dust dispersal in mines become available.

²⁰Singer, J. M., E. B. Cook, and J. Grumer. Equivalences and Ignition Limits of Coal Dust and Methane Mixtures. BuMines RI 6931, 1967, 35 pp.

TABLE 5. - Surface lifting of top 0.32 cm of coal layer and line source lifting of underlying 1.25 cm of rock dust layer

($k_{dust} = 100 \text{ cm}^2/\text{sec}$, $U = 50 \text{ m/sec}$, duct height and width = 53.2 cm; dust concentration in mg/liter)

z\ t, cm	0.1 sec		0.2 sec		0.3 sec		0.5 sec		1.0 sec	
	Coal	Rock	Coal	Rock	Coal	Rock	Coal	Rock	Coal	Rock
25	8.8	440	1.0×10^{-9}	9.6×10^3	0	8.9×10^4	0	0	0	0
50	33	240	12	5.9×10^3	13	4.4×10^4	0	0	0	0
100	19	100	14	3.3×10^3	41	2.4×10^4	0	0	0	0
200	11	22	20	1.4×10^3	30	1.2×10^4	0	0	0	0
400	7.7	0.15	14	290	21	3.9×10^3	0	2.8×10^{-11}	0	0
800	0	0	2.3	2.0	2.5	400	0	1.8×10^{-15}	0	0
1600	0	0	0	0	0	0	6.1	750	0	0
$x = 10 \text{ cm}$										
25	1.7×10^{-10}	6.2×10^{-10}	1.5×10^{-20}	1.1×10^{-8}	0	4.4×10^{-8}	0	0	0	0
50	3.8×10^{-9}	3.6×10^{-9}	1.8×10^{-10}	3.2×10^{-8}	5.1×10^{-9}	6.0×10^{-8}	0	0	0	0
100	3.4×10^{-6}	4.0×10^{-4}	3.3×10^{-5}	1.1×10^{-2}	1.0×10^{-4}	2.0×10^{-2}	0	0	0	0
200	1.7×10^{-2}	4.2×10^{-2}	3.1×10^{-2}	2.7	4.7×10^{-2}	18	0	0	0	0
400	0.31	6.6×10^{-3}	0.55	13	0.83	170	0	5.9×10^{-12}	0	0
800	0	0	0.47	0.42	0.50	83	0	4.1×10^{-16}	0	0
1600	0	0	0	0	0	0	2.8	340	0	0
$x = 20 \text{ cm}$										
25	1.7×10^{-9}	1.1×10^{-10}	2.5×10^{-20}	3.3×10^{-9}	0	7.3×10^{-8}	0	0	0	0
50	4.8×10^{-9}	2.1×10^{-10}	3.0×10^{-9}	2.9×10^{-9}	1.7×10^{-9}	1.1×10^{-9}	0	0	0	0
100	1.2×10^{-9}	1.5×10^{-10}	3.0×10^{-10}	3.0×10^{-9}	1.5×10^{-9}	5.5×10^{-9}	0	0	0	0
200	1.1×10^{-9}	2.6×10^{-10}	2.9×10^{-9}	1.6×10^{-8}	4.3×10^{-9}	4.7×10^{-8}	0	0	0	0
400	2.0×10^{-5}	5.5×10^{-7}	3.4×10^{-5}	1.1×10^{-3}	5.1×10^{-5}	1.3×10^{-5}	0	5.7×10^{-18}	0	0
800	0	0	3.9×10^{-3}	3.8×10^{-3}	3.9×10^{-3}	0.77	0	4.3×10^{-18}	0	0
1600	0	0	0	0	0	0	0.27	33	0	0

TABLE 6. - Surface dispersal of mixture of 65 percent rock dust and 35 percent coal dust

($k_{\text{rock dust}} = 50 \text{ cm}^2/\text{sec}$, $k_{\text{coal dust}} = 100 \text{ cm}^2/\text{sec}$,
 $U = 50 \text{ m/sec}$, duct height = 4 m, duct width = 6 m,
length of dust bed = 3 m, width of dust bed = 6 m;
dust concentration in mg/liter)

z \ t, cm	0.1 sec		0.2 sec		0.3 sec		0.5 sec		1.0 sec	
	Coal	Rock	Coal	Rock	Coal	Rock	Coal	Rock	Coal	Rock
$x = 0$										
25	620	2.5×10^3	1.4×10^4	5.2×10^{-3}	1.2×10^5	4.1×10^5	0	0	0	0
50	350	1.4×10^3	8.4×10^3	3.4×10^4	2.1×10^{-4}	3×10^{11}	0	0	0	0
100	150	600	4.7×10^3	1.9×10^4	3.4×10^4	1.4×10^5	0	0	0	0
200	31	130	2.0×10^3	8.0×10^3	1.7×10^4	6.7×10^4	0	0	0	0
400	0	0	420	1.7×10^3	5.5×10^3	2.2×10^4	1.7×10^5	6.8×10^5	0	0
800	0	0	2.6	11	570	2.3×10^3	2.9×10^4	1.2×10^5	0	0
1600	0	0	0	0	0	0	1.2×10^3	4.7×10^3	0	0
$x = 10 \text{ cm}$										
25	2.9×10^{-4}	0.1	1.2×10^{-2}	4.5×10^{-7}	9.2	88	0	0	0	0
50	2.9×10^{-7}	6.1×10^{-4}	4.8×10^{-6}	1.9×10^{-2}	1.2×10^{-11}	5.4×10^{-16}	0	0	0	0
100	5.7×10^{-4}	4.4×10^{-7}	1.6×10^{-2}	1.4×10^{-5}	2.9×10^{-2}	7.7×10^{-6}	0	0	0	0
200	6.0×10^{-2}	4.7×10^{-4}	7.8	2.9×10^{-2}	25	0.16	0	0	0	0
400	0	0	18	3.2	240	41	2.1×10^3	100	0	0
800	0	0	0.54	0.49	120	100	5.6×10^3	4.5×10^3	0	0
1600	0	0	0	0	0	0	530	980	0	0
$x = 20 \text{ cm}$										
25	5.9×10^{-5}	1.0×10^{-3}	2.3×10^{-3}	2.4×10^{-6}	0.55	22	0	0	0	0
50	5.9×10^{-8}	1.3×10^{-4}	1.6×10^{-6}	3.9×10^{-3}	2.8×10^{-12}	7.2×10^{-17}	0	0	0	0
100	4.5×10^{-6}	1.7×10^{-7}	1.9×10^{-6}	7.1×10^{-6}	1.4×10^{-5}	2.0×10^{-5}	0	0	0	0
200	2.2×10^{-6}	4.3×10^{-8}	1.4×10^{-6}	3.1×10^{-6}	8.2×10^{-6}	3.9×10^{-5}	0	0	0	0
400	0	0	1.5×10^{-3}	1.2×10^{-2}	1.9×10^{-2}	1.6×10^{-5}	4.0×10^{-3}	6.7×10^{-5}	0	0
800	0	0	4.9×10^{-3}	4.1×10^{-5}	1.1	8.4×10^{-3}	44	0.26	0	0
1600	0	0	0	0	0	0	51	9.0	0	0

SUMMARY

A method is given for computing dust concentrations in a turbulent gas stream following explosion-induced entrainment of dust beds on mine surfaces. The dust concentrations from different source locations (floor, roof, and ribs) are additive, as are the concentrations from different entrainment rates of either stationary or moving sources. Both rectangular and circular ducts are considered. Solutions are given for several cases, assuming diffusion coefficients in the range of 25 to 100 cm²/sec, and using the rates of entrainment determined in explosion tunnel experiments. The treatment is extended to the prediction of in-flight coal and rock dust concentrations in coal mine passageways for which there are no measured observations.

APPENDIX.--LIST OF SYMBOLS

a	= Radius of circular duct.
	= Height of rectangular duct.
b	= Width of rectangular duct.
c	= Dust concentration, milligrams per liter air.
g	= Acceleration of gravity.
h	= Dust-bed height.
k	= Diffusion coefficient.
L	= Dust-bed length in axial direction.
M,N	= Constants defined in equation 11.
n	= Distance in the direction normal to a boundary.
Q	= Mass of dust production.
Q_s	= Mass rate of dust production from a surface source.
r	= Radial coordinate.
Re	= Reynolds number.
t	= Time.
t_d	= Time at which dust-lifting process is completed.
U	= Convection velocity.
U_x	= Friction velocity.
x,y,z	= Cartesian coordinates (x, y, and z are height from floor, distance from side wall, and downstream distance, respectively).
Z	= Parameter in coordinate transformation. $Z = z - Ut$
α	= Positive roots defined by equation 8.
e	= Eddy diffusivity.
θ	= Angle.
θ_0	= Parameter of dust-bed configuration defined in figure 3.

- ρ = Bulk density of dust bed.
- $\phi(t_1)$ = Rate of mass released instantaneously from a surface at time t_1 .
- τ = Time required to disperse the entire dust bed.
- ν = Kinematic viscosity.

Subscripts

- 1 = Location of instantaneous source.